Since January 2020 Elsevier has created a COVID-19 resource centre with free information in English and Mandarin on the novel coronavirus COVID-19. The COVID-19 resource centre is hosted on Elsevier Connect, the company's public news and information website.

Life Sciences 263 (2020) 118564

Contents lists available at ScienceDirect

Life Sciences

journal homepage: www.elsevier.com/locate/lifescie

DEFA1B inhibits ZIKV replication and retards cell cycle progression through interaction with ORC1

Shuang Li[a], Anjing Zhu[a], Kai Ren[a], Shilin Li[a], Limin Chen[a,b,*]

[a] Provincial Key Laboratory for Transfusion-Transmitted Infectious Diseases, Institute of Blood Transfusion, Chinese Academy of Medical Sciences and Peking Union Medical College, Chengdu, Sichuan 610052, China
[b] Toronto General Research Institute, University of Toronto, ON M5G 1L6, Canada

ARTICLE INFO

Keywords:
Zika virus (ZIKV)
Exosomes
Defensins
Defensin alpha 1B (DEFA1B)
Cell cycle

ABSTRACT

Aims: Zika virus (ZIKV) infection causes a public health concern because of its potential association with the development of microcephaly. During viral infections, the host innate immune response is mounted quickly to produce some endogenous functional molecules to limit virus replication and spread. Exosomes contain molecules from their cell of origin following virus infection and can enter recipient cells for intercellular communication. Here, we aim to clarify whether ZIKV-induced exosomes can regulate viral pathogenicity by transferring specific RNAs.

Main methods: In this study, exosomes were isolated from the supernatants of A549 cells with or without ZIKV infection. Human transcriptome array (HTA) was performed to analyze the profiling of RNAs wrapped in exosomes. Then qPCR, western blotting and ELISA were used to determine ZIKV replication. CCK-8 and flow cytometry were used to test the cell proliferation and cell cycles. Co-culture assay was used to analyze the effect of exosomes on the cell cycles of recipient cells.

Key findings: Through human transcriptome array (HTA) we found the defensin alpha 1B (DEFA1B) expression was significantly increased within exosomes isolated from ZIKV infected A549 cells. Additionally, we found that the extracellular DEFA1B exerts significant anti-ZIKV activity, mainly before ZIKV entering host cells. Interestingly, up-regulated DEFA1B retards the cell cycle of host cells. Further studies demonstrated that DEFA1B interacted with the origin recognition complex 1 (ORC1) which is required to initiate DNA replication during the cell cycle and increased DEFA1B expression decreased the ORC1 level in the cell nuclei. Accordingly, DEFA1B-containing exosomes can be internalized by the recipient cells to retard their cell cycles.

Significance: Together, our results demonstrated that the anti-ZIKV activity of DEFA1B can be mediated by exosomes, and DEFA1B interacts with ORC1 to retard cell cycles. Our study provides a novel concept that DEFA1B not only acts as an antiviral molecule during ZIKV infection but also may correlate with cell proliferation by retarding the progression of cell cycles.

1. Introduction

Zika virus (ZIKV) is a re-emerging arbovirus that belongs to the Flaviviridae family and is transmitted by infected Aedes mosquitoes. ZIKV is a single positive-stranded RNA virus with a genome size of approximately 10.8 kilobases [1]. ZIKV infection emerged as a public health concern after increasing evidence linking ZIKV infection with the potential development of microcephaly [2]. Although previous study alluded that ZIKV could directly infect human neural progenitor cells (hNPCs) to induce cell death and disturb cell cycle progression to affect human brain development [3], the detailed underlying molecular mechanism remains elusive.

In the battle between pathogens and hosts, the production of endogenous defensins is one of the first lines of protection for the host. Various types of human cells can produce defensins that have broad antimicrobial activity to many pathogens, including bacteria, viruses and fungi [4,5]. Defensins have been shown to protect against many virus infections, such as human immunodeficiency virus (HIV), influenza A virus (IAV), human adenovirus (HAdV), severe acute respiratory syndrome coronavirus (SARSC), papillomavirus (HPV), respiratory syncytial virus (RSV), and herpes simplex virus (HSV) [6,7]. Currently, no approved vaccines or therapies are available for the prevention and

* Corresponding author at: Provincial Key Laboratory for Transfusion-Transmitted Infectious Diseases, Institute of Blood Transfusion, Chinese Academy of Medical Sciences and Peking Union Medical College, Chengdu, Sichuan 610052, China.
E-mail addresses: alyssa@bjmu.edu.cn (S. Li), limin_chen_99@yahoo.com (L. Chen).

https://doi.org/10.1016/j.lfs.2020.118564
Received 25 June 2020; Received in revised form 22 September 2020; Accepted 1 October 2020
Available online 17 October 2020
0024-3205/

treatment of ZIKV infection, therefore defensins may be a promising drug target for the treatment of ZIKV infection.

The 'origin recognition complex' (ORC), as one of the most important complexes in all eukaryotes, is involved in the initiation of DNA replication and has been linked to various diseases [8]. Although ORC consists of ORC1–6, ORC1 is the biggest subunit that is necessary for the initiation of DNA replication [9]. Notably, several reports linked ORC to numerous human diseases [10,11]. Of particular interest, mutations in ORC1 have been shown to cause Meier-Gorlin syndrome, which is characterized by microcephaly and primordial dwarfism [12,13].

Recent work has pointed out that exosomes function as crucial regulators of cellular cross-talk. Exosomes are phospholipid bilayer-bound structures that can transfer packed mRNA, miRNA, and/or proteins into recipient cells to facilitate intercellular communications and to affect gene expression in recipient cells [14,15]. In addition, emerging evidence indicated that exosomes can mediate the transfer of pathogen-derived antigens and virulence factors [16]. Exosomes play various roles in the pathogenesis of ZIKV. For example, ZIKV can be wrapped into a sort of cargo of the placental exosomes and be transmitted through exosomes into trophoblast cells [17]. Furthermore, exosomes have been shown to mediate ZIKV transmission through SMPD3 neutral Sphingomyelinase in cortical neurons [18].

In order to further decipher the role of exosomes in the pathogenesis of ZIKV infection, we used human transcriptome array (HTA) and bioinformatics analysis to identify candidate molecules in ZIKV-induced exosomes. We identified defensin alpha 1B (DEFA1B) is involved in ZIKV infection and pathogenesis. Our data demonstrated that DEFA1B not only inhibits ZIKV replication before ZIKV entering host cells but also retards the progression of cell cycles through interaction with ORC1. Interestingly, the function of DEFA1B to retard cell cycle progression can be transmitted by ZIKV-induced exosomes. In conclusion, these findings describe the double effects of ZIKV-induced DEFA1B: 1) as an antiviral peptide to inhibit ZIKV infection; 2) as an ORC1-binding protein to retard the progression of cell cycle which may be linked to the microcephaly manifestation following ZIKV infection.

2. Materials and methods

2.1. Cells and virus

Human adenocarcinoma alveolar basal epithelial cell line (A549), human embryonic kidney epithelial cell line (HEK293T) and undifferentiated human neuroblastoma SH-SY5Y cell line were cultured in DMEM (HyClone Laboratories, USA) supplemented with 10% fetal bovine serum (FBS; Biological Industries, Israel), 100 IU/mL penicillin, and 100 μg/mL streptomycin at 37 °C with 5% (v/v) CO_2 in a humidified incubator. Before exosomes isolation, the A549 cells, with a confluence of about 60–70%, were grown for 48 h in DMEM supplemented with exosome-depleted FBS (Gibco, USA). A549 cells were infected by ZIKV GZ01 strain at a multiplicity of infection (MOI) of 0.5 in DMEM medium supplemented with 2% FBS. Cell cycle arrest was induced by the double-thymidine block method, and HEK293T cells were incubated in the presence of 2.5 mM thymidine for two periods of 18 h with an interval incubation of 9 h in the absence of thymidine. Synchronous growth following arrest was achieved by two washes with PBS and subsequent culturing without thymidine.

2.2. Exosomes isolation

After A549 cells were infected with or without ZIKV for 48 h, the culture medium was harvested and subjected to sequential centrifugation steps (300 ×*g* for 5 min; 2000 × g for 15 min; 10,000*g* for 60 min at 4 °C) to remove dead cells, cellular debris, microvesicles and membrane debris. The supernatants were further centrifuged at 100,000 ×*g* for 90 min at 4 °C, followed by sucrose density gradient purification to purify exosomes [19]. After that, final pellets of exosomes were re-suspended in PBS to 1/2000th of the original volume of the culture supernatant, and small aliquots were stored at −80 °C freezer until use.

2.3. Characterization of the isolated exosomes

Western blot analysis was carried out according to the standard procedure. Antibodies of anti-human CD63, CD81, TSG101 were obtained from Santa Cruz (CA, USA), and Calnexin obtained from CST (MA, USA). Secondary goat anti-rabbit and goat anti-mouse antibodies were also obtained from CST (MA, USA). BIO-RAD ChemiDoc Imaging System (Rio-Rad, USA) was used to quantify the band density. The size and particle number of the purified exosomes were analyzed using Zeta View (Particle Metrix GmbH, Germany). Exosomes preparations were further verified by electron microscopy (Tecnai Spirit Bio-Twin, USA).

2.4. RNA isolation and microarray analysis

Total exosomes RNAs were isolated using Trizol (Life Technologies, USA) and Dr. GenTLE™ Precipitation Carrier (Takara, Japan) according to the manufacturer's guidelines. RNA was quantified using Nanodrop ND-1000 (Thermo Fisher Scientific, USA). The integrity of these total RNAs was assessed using Agilent 2100 Bioanalyzer (Agilent, USA). The mRNA and lncRNA array profiling was performed by using the Affymetrix GeneChip HTA 2.0 (Affymetrix, USA). With this array, it was possible to evaluate > 285,000 full-length transcripts, > 245,000 coding transcripts, > 40,000 non-coding transcripts, and > 339,000 probe sets covering exon-exon junctions.

2.5. Real-time quantitative PCR (RT-qPCR)

Quantitative PCR analysis of DEFA1B, ZIKV and GAPDH was carried out by using a Bio-Rad CFX96 (Bio-Rad Laboratories, USA) with SYBR-Green PCR Master Mix (Nanoprotein, China) according to the manufacturer's protocol. Samples were run in triplicate and at least 3 independent experiments were performed. Analysis of relative gene expression was performed by the $2^{-\Delta\Delta CT}$ method. Data are presented as mean ± SD. A p value of < 0.05 was considered to be statistically significant. The primers for RT-qPCR used in the present study are listed as follows. For GAPDH, the forward primer was 5′-GCCTCCTGCACCA CCAACTG-3′ and the reverse primer was 5′-ACGCCTGCTTCACCACC TTC-3′; for DEFA1B, the forward primer was 5′-CACTCCAGGCAAGAG CTGAT-3′ and the reverse primer was 5′-TCTGCAATAGCAGGCCA TGT-3′; for ZIKV, the forward primer was 5′-GCAGAGCAACGGATGG GATA-3′ and the reverse primer was 5′-ATGGTGGGAGCAAAACG GAA-3′.

2.6. Plasmid construction and verification of protein expression

Plasmids expressing DEFA1B were constructed with routine molecular cloning techniques. The full length human DEFA1B gene was amplified by polymerase chain reaction (PCR) from total RNA isolated from A549 cells and cloned into pcDNA3.1-T2A-EGFP vector to create the mammalian expression plasmids pcDNA3.1-DEFA1B-T2A-EGFP. All the constructs were sequence-verified. The plasmids were transiently transfected into HEK293T cells using Lipofectamine 3000 (Invitrogen, USA) and protein expression was verified by Western Blot (WB) using DEFA1B-specific antibody and secreted DEFA1B into the culture medium was assessed by an ELISA kit (Cloud-Clone Corp, USA). Concentrations of human DEFA1B were determined by plotting the absorbance of each sample against a standard curve of recombinant human DEFA1B.

2.7. DEFA1B anti-viral activity

A549 and HEK293T cells were cultured in plates and allowed to attach overnight, infected with ZIKV GZ01 strain at MOI of 0.5, in

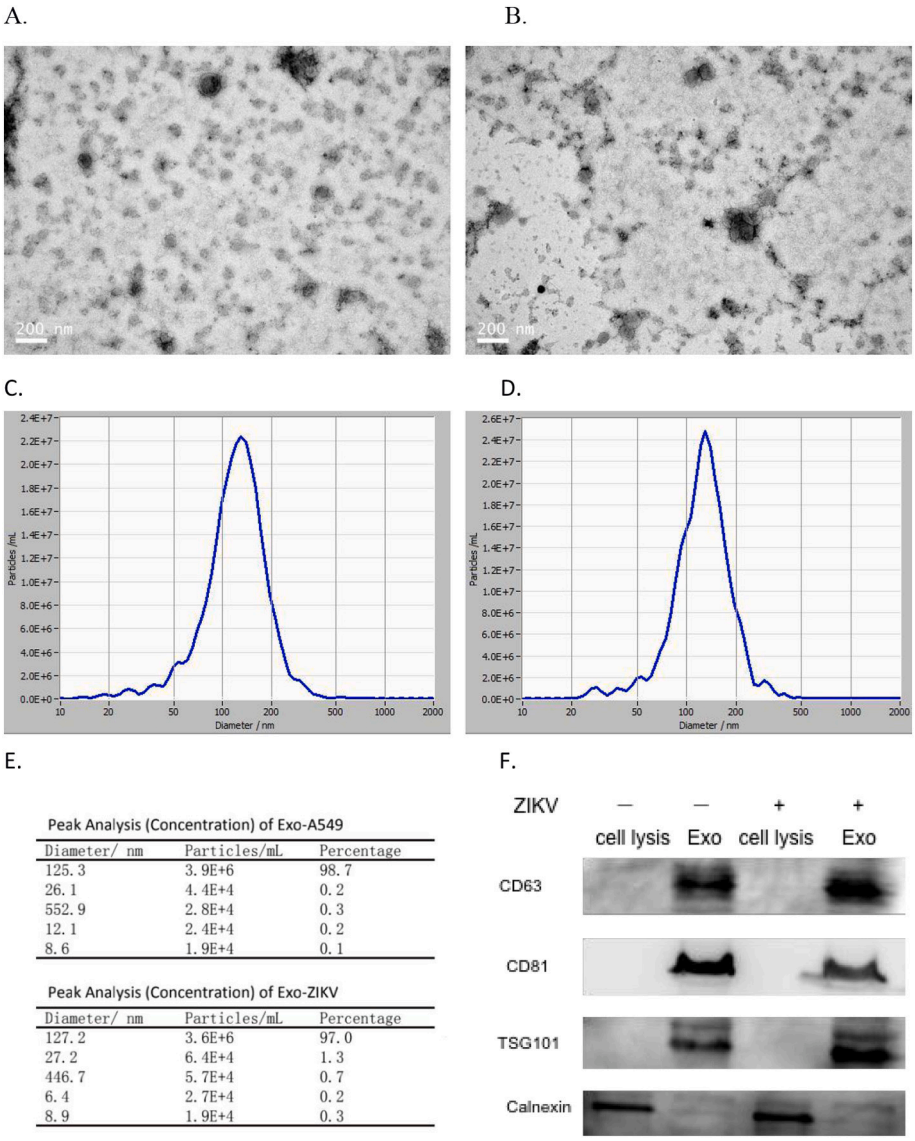

Peak Analysis (Concentration) of Exo-A549

Diameter/ nm	Particles/mL	Percentage
125.3	3.9E+6	98.7
26.1	4.4E+4	0.2
552.9	2.8E+4	0.3
12.1	2.4E+4	0.2
8.6	1.9E+4	0.1

Peak Analysis (Concentration) of Exo-ZIKV

Diameter/ nm	Particles/mL	Percentage
127.2	3.6E+6	97.0
27.2	6.4E+4	1.3
446.7	5.7E+4	0.7
6.4	2.7E+4	0.2
8.9	1.9E+4	0.3

Fig. 1. Characterization of exosomes isolated from A549 cells (Exo-A549) or ZIKV infected A549 cells (Exo-ZIKV). Transmission electron micrograph of Exo-A549 (A) and Exo-ZIKV (B). Nanoparticle tracking analysis of exosomes indicated Exo-A549 particles sizes median diameter of 125.3 nm (C) and Exo-ZIKV median size diameter of 127.2 nm (D). Peak analysis of exosomes (E). Western blotting of exosomes was performed to confirm the presence of exosomal marker protein, CD63, CD81 and TSG101. Absence the endoplasmic reticulum protein, Calnexin, in exosomes but was detectable in whole cell lysates (F).

DMEM with DEFA1B for 2 h to allow virus adsorption. Then cells were washed twice with PBS and cultured with complete medium. Cells were cultured at 37 °C and 5% CO_2 for 48 h, then cells were harvested to test ZIKV copies and NS1 expression.

2.8. Subcellular fractionation

Cytoplasmic and nuclear proteins of the cells were separated by using the Membrane Nuclear and Cytoplasmic Protein Extraction kit (Sangon, China), following the manufacturer's instructions. In brief, after washing the cells with PBS, cells were lysed with ice-cold Lysis buffer A for 20 min, and the cell lysates were centrifuged at 13,000*g* for 10 min, after which the cytoplasmic proteins were located in the supernatant and collected. Ice-cold lysis buffer B was then added to the pellets for 10 min, and the cell lysates were centrifuged at 13,000*g* for 10 min, after which the nuclear proteins were located in the supernatant and collected.

2.9. Western blot

Total cellular proteins were lysed with RIPA lysis buffer (1% NP-40, 1% Triton X-100, 1 mM MgCl2, 0.1% SDS, and 10 mM Tris-HCl, pH 7.4) and quantified by BCA method before being separated by SDS-PAGE. Western blot analysis was carried out according to the standard procedures. Primary antibodies of CD63, CD81, TSG101, DEFA1B and ORC1 were obtained from Sigma-Aldrich (St Louis, MO, USA), and antibodies of Calnexin, NS1, PARP and GAPDH were obtain from CST (MA, USA), DEFA1B antibody was from proteintech (IL, USA). Secondary antibodies goat anti-rabbit, goat anti-mouse and goat anti-rat were also obtained from CST (MA, USA). Bio-rad Image Acquisition and Analysis Software (UVP, Upland, CA, USA) were performed to quantify the band density.

2.10. Cell Counting Kit-8 (CCK-8)

Cell proliferation and viability were evaluated using a CCK-8 assay (TransGene Biotech, China). For CCK8, the cells were allowed to grow

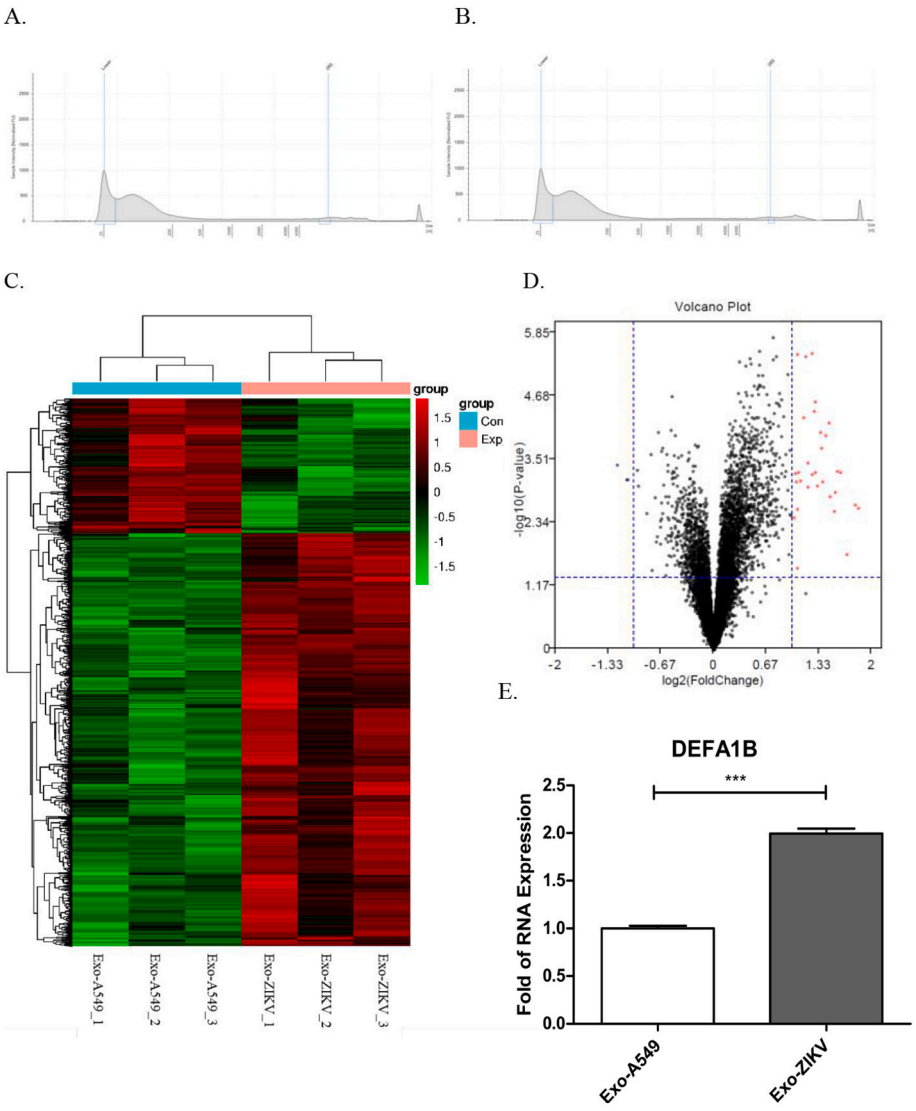

Fig. 2. Profiling of RNAs led to the discovery of distinct signatures for Exo-A549 and Exo-ZIKV subsets. RNA profiles of Exo-A549 (A) and Exo-ZIKV (B) both lack the two rRNA peaks (18 s and 28 s) and are enriched in short RNAs. (C) Heatmap reflective of coding and noncoding RNAs which log FC ≥ 0.3 and log FC ≤ -0.3, with p value < 0.05. (D) Volcano map of RNAs. (E) Exosomal RNAs were isolated and RT-qPCR used to determine the relative expression of DEFA1B and normalized to GAPDH. Significance was determined by Student unpaired t-test $^{***}p < 0.001$.

in a 96-well plate, at the concentration of 5000 cells per well. At each time point, cells were rinsed with 1/10 CCK-8 diluted in DMEM for 1.5 h, and the optical density of the cellular homogenate was measured at 450 nm. Each experiment was performed in quintuplicate.

2.11. Flow cytometry analysis

The effect of DEFA1B on cell proliferation was evaluated by measuring the distribution of the cells in the different phases of the cell cycle by flow cytometry. This determination was based on the measurement of the DNA content of nuclei labeled with propidium iodide (PI). Cells were prepared by trypsinization and washed twice with phosphate-buffer saline (PBS), and fixed in 70% ethanol overnight. Staining for DNA content was performed with 50 μg/mL propidium iodide (PI, Solaribio, China) and 1 mg/mL RNase A (Solaribio, China) for 30 min. The analysis was performed on a BDCalibur flow cytometer (Becton Dickinson, USA) with Cell Quest Pro software. Cell-cycle modeling was performed with Modfit 5.0 software (Verity Software House, USA).

2.12. Co-immunoprecipitation

Co-immunoprecipitation (co-IP) was performed on lysates from HEK293 cells transfected with pcDNA3.1-DEFA1B-T2A-EGFP or control plasmid. Anti-DEFA1B antibody (proteintech, USA) and Protein A&G Agarose (Santa Cruz Biotechnology) were used in this co-IP assay. The immunoprecipitates were washed five times and separated by 10% SDS–PAGE gel electrophoresis and blotted using anti-DEFA1B and anti-ORC1 (Santa Cruz), respectively.

2.13. Exosomes uptake into recipient cells

PKH67 Green Fluorescent Cell Linker Kit (Sigma) was used to label exosomes according to the manufacturer's protocol. Briefly, exosomes were re-suspended in 500 μL Diluent C. In addition, 2 μL PKH67 was mixed with 1 mL Diluent C, followed by mixing with the exosomes suspension and incubated for 4 min. To stop the labeling reaction, an equal volume of 1% BSA was added into the mixed solution. Then, the labeled exosomes were ultracentrifuged at 100,000 × g for 1 h at 4 °C, washed with 1 × PBS, and ultracentrifuged again. To detect exosomes uptake into recipient cells, HEK293T cells and SH-SY5Y cells were

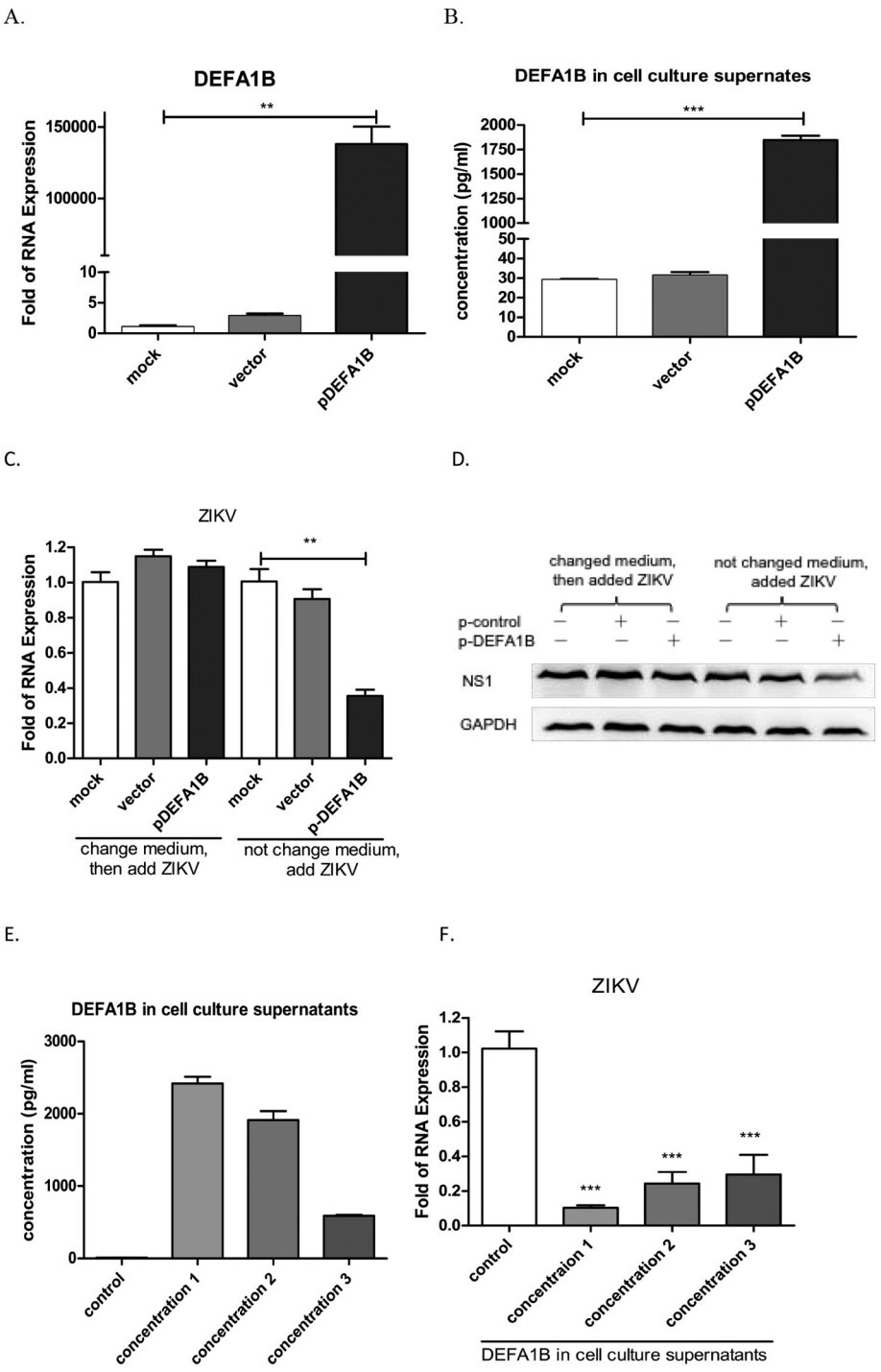

Fig. 3. The anti-ZIKV effect of DEFA1B. Here, cells with treatments (for 48 h): no treatment (mock), pcDNA3.1-T2A-EGFP (vector) and pcDNA3.1-DEFA1B-T2A-EGFP plasmid (pDEFA1B), as presented in the bar diagrams. All experiments were performed in triplicates. After transfected with plasmid, qPCR (A) and ELISA (B) were used to determinate the expression level of DEFA1B. Then infected with ZIKV, both mRNA (C) and protein (D) levels showed DEFA1B in culture supernatants can inhibit ZIKV replication. To further analysis the anti-ZIKV effect of extracellular DEFA1B, we put three different concentration of DEFA1B in the culture supernatants (E) then infected with ZIKV, qPCR (F) and western bolt (G) were used to determinate ZIKV replication. The changes of ZIKV copies in medium with or without DEFA1B from 0 to 6 h (H). Also, we verified the anti-ZIKV effect of intracellular DEFA1B, three different RNA (I) and protein (J) levels of DEFA1B in cells, before infected with ZIKV change medium with fresh medium without DEFA1B. Use qPCR (K) and western blot (L) to analysis ZIKV level.

grown in 24-well plates at a density of 1×10^4 cells per well and PKH67-labeled exosomes were diluted in whole-medium solution and was added into each well. Cells were cultured for 6 h at 37 ˚C. DAPI was used to stain the nucleus, and the cells were observed using fluorescence microscope (Olympus IX71, Germany).

2.14. Statistical analysis

Student's *t*-tests were used to analyze the differences between groups. All experiments were repeated at least three times. The *p*-value < 0.05 was considered statistically significant ($*p < 0.05$; $**p < 0.01$; $***p < 0.001$).

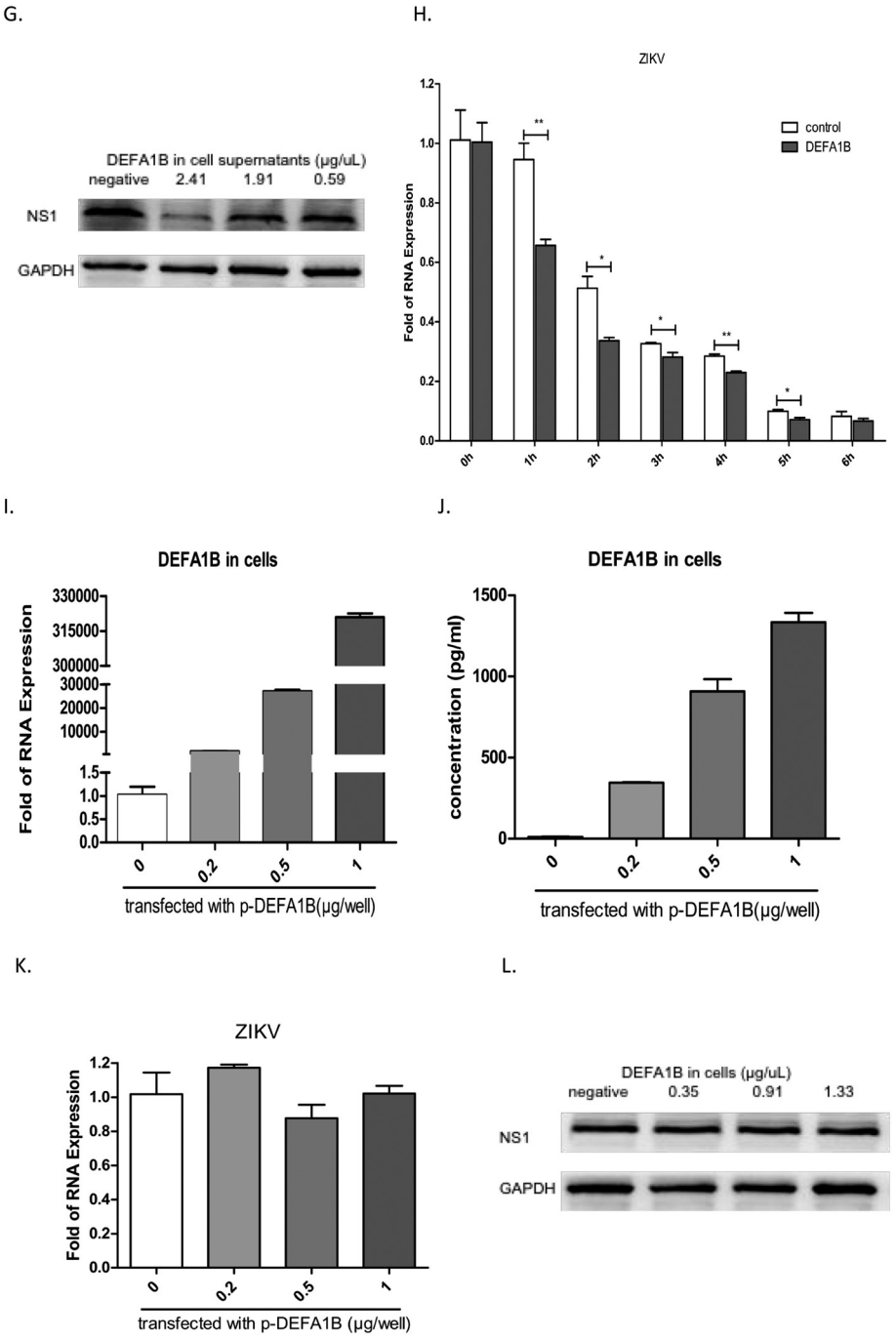

Fig. 3. (*continued*)

3. Results

3.1. Identification and characterization of exosomes derived from A549 cells and ZIKV infected A549 cells

Purified exosomes from the culture supernatants of A549 cells with or without ZIKV infection were examined by transmission electron microscopy (TEM). Membrane-bound round-shaped vesicles ranged in size from 100 to 200 nm in diameter were shown (Fig. 1A, B). Furthermore, nanoparticle tracking analysis (NTA) indicated that the mean diameters of 98.7% Exo-A549 are 125.3 nm, and 97% of Exo-ZIKV is 127.2 nm (Fig. 1C, D, E). Western blot revealed that the exosome-specific proteins, CD63, CD81 and TSG101, were enriched in all exosomes samples but not in cell lysates–confirming these vesicles are indeed exosomes. Calnexin, an endoplasmic reticulum protein, was detectable in whole-cell lysates but not in the exosomes, indicating that the exosomes preparations were not contaminated with other vesicles (Fig. 1F). Together, these results confirmed the isolated vesicles are indeed purified exosomes and the isolation method is reliable.

3.2. Differential gene expression profiling between exosomes isolated from ZIKV infected A549 and A549 control cells

To analyze whether ZIKV infection-induced exosomes contain epigenetic regulators to influence viral infection and the behavior of target cells, human transcriptome array 2.0 analysis was performed on the total RNAs extracted from exosomes derived from A549 cells infected with ZIKV (Exo-ZIKV) or exosomes extracted from A549 control cells

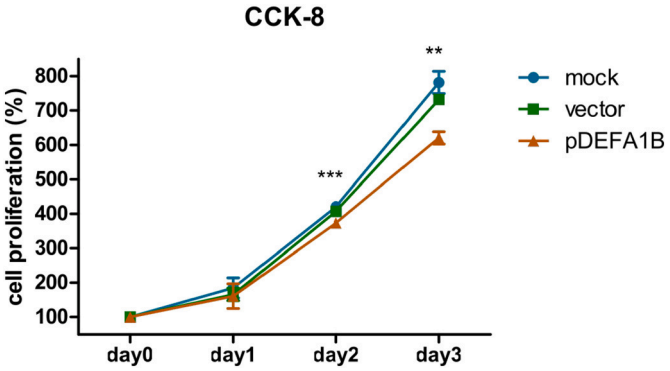

Fig. 4. DEFA1B retards cell cycles. The CCK8 assay used to evaluate the proliferation of the HEK293T cells after transfection with the pcDNA3.1-DEFA1B-T2A-EGFP plasmid (pDEFA1B) or pcDNA3.1-T2A-EGFP (vector) or no transfection (mock).

(Exo-A549). The profile of RNAs in exosomes is fundamentally different to that of the RNA in cells. 18S and 28S rRNA subunits were present in cells, but RNA isolated from exosomes mainly contained small RNAs without or with little rRNAs. The RNA profiles of both Exo-A549 (Fig. 2A) and Exo-ZIKV (Fig. 2B) lacked the two rRNA peaks (18S and 28S) and the short RNAs were enriched. This indicates the total RNA extracted is exosomes origin and the isolation method is quality assured. Heatmap analysis showed that Exo-A549 samples were clustered together and they are separated from Exo-ZIKV samples. Fold changes of RNAs expression from Exo-ZIKV compared with Exo-A549 were represented in the heatmap (Fig. 2C). Fold change log FC ≥ 1.0 and log FC ≤ -1.0, with p value < 0.05 was considered statistically significant. All RNAs with statistically significant fold changes were presented in red color in the volcano map (Fig. 2D). Among those differentially-expressed genes, DEFA1B was identified. The mRNA level of DEFA1B was up-regulated within Exo-ZIKV compared with Exo-A549. Then, we used qPCR to verify the expression levels of DEFA1B in exosomes. As expected, the qPCR data were in line with the HTA data, that DEFA1B levels were significantly increased in Exo-ZIKV compared with Exo-A549 (Fig. 2E). To further analyze the effect of DEFA1B on ZIKV infection, we created the mammalian expression plasmid pcDNA3.1-T2A-EGFP and pcDNA3.1-DEFA1B-T2A-EGFP (Supplementary material), and we confirmed the transfection efficiency by using a fluorescence microscope to measure GFP fluorescence. Our data showed the plasmid can be efficiently transfected into 293T cells without affecting the cell survival rate.

3.3. The extracellular DEFA1B significantly inhibits ZIKV replication

48 h after the plasmids transfection, the mRNA level of DEFA1B was significantly up-regulated (Fig. 3A). ELISA data showed the DEFA1B could be secreted into culture supernatants, and the concentration of DEFA1B was significantly increased compared with the control group (Fig. 3B). Furthermore, to examine the anti-viral ability of DEFA1B, we divided the cells into two groups: in one group the supernatants were removed and replaced with fresh medium; the other group the supernatants that contain DEFA1B were added. Then, these two groups of cells were infected with ZIKV at MOI = 0.5. Our data showed that DEFA1B contained in culture supernatants significantly inhibited ZIKV replication at mRNA level (Fig. 3C). NS1 (which is the non-structural protein 1 of ZIKV) expression level was also significantly decreased in the group with DEFA1B in culture supernatants (Fig. 3D). To further analyze the anti-ZIKV effect of extracellular DEFA1B, we added three different concentrations (2418.1 ± 102.9 pg/mL, 1913.9 ± 92.1 pg/mL, 588.7 ± 31.0 pg/mL) of DEFA1B to the supernatants of HEK293T cells (Fig. 3E) and infected the cells with ZIKV. Compared with no DEFA1B in supernatants, qPCR data showed that ZIKV replication was significantly inhibited in a dose-dependent manner (Fig. 3F). We also verified the same tendency at the viral protein levels using western blot (Fig. 3G). Furthermore, we compared the changes of ZIKV copies in medium with or without DEFA1B to further validate the anti-ZIKV effect of extracellular DEFA1B. The qPCR data showed the ZIKV copies were significantly decreased in medium with DEFA1B when compared with those in normal medium (without DEFA1B) (Fig. 3H). Furthermore, we compared the changes of ZIKV copies in medium with or without DEFA1B to further validate the anti-ZIKV effect of extracellular DEFA1B. The qPCR data showed the ZIKV copies were significantly decreased in medium with DEFA1B when compared with those in normal medium (without DEFA1B) (Fig. 3H). In order to test whether the intracellular DEFA1B has anti-ZIKV activity, we transfected different doses (0.2 μg, 0.5 μg and 1 μg per well) of pcDNA3.1-DEFA1B-T2A-EGFP plasmids into HEK293T cells. qPCR (Fig. 3I) and ELISA (Fig. 3J) data showed the DEFA1B was indeed up-regulated in HEK293T cells after transfection. We then replaced the culture supernatants with fresh medium and infected the cells with ZIKV (MOI = 0.5). Both qPCR (Fig. 3K) and western blot (Fig. 3L) data showed no significant changes of ZIKV replication between untreated HEK293T cells and cells with up-regulated DEFA1B group.

3.4. DEFA1B inhibits cell proliferation

During our research we found that up-regulated DEFA1B expression in HEK293T reduced the cell growth rate. So we used CCK8 to investigate the proliferation of HEK293T cells transfected with pcDNA3.1-DEFA1B-T2A-EGFP or with control vector, and we found that compared with untreated or blank vector control group, the proliferation of cells were obviously decreased at day 2 and day 3 after transfected with pcDNA3.1-DEFA1B-T2A-EGFP (Fig. 4).

3.5. DEFA1B arrests ORC1 to enter into nucleus to retard cell cycle progression

Proteins often do not just function as a single substance but rather as team players in a dynamic network. Growing evidence shows that protein–protein interactions are crucial in many biological processes in living cells. The database STRING (https://string-db.org/) is a precomputed global resource for the exploration and analysis of these associations. We found that DEFA1B was the hub of ORC1 interaction that is the largest subunit of the ORC (Fig. 5A); therefore, we decided to focus further analysis on ORC1. To confirm whether DEFA1B specifically interacts with ORC1, immunoblot analysis of whole cell lysates and anti-DEFA1B affinity immunoprecipitation (IP) derived from 293T cells transfected with pcDNA3.1-DEFA1B-T2A-EGFP or blank vector control plasmid were performed. Co-IP assay clearly demonstrated that DEFA1B interacts with ORC1 (Fig. 5B). We further analyzed the expression levels of ORC1 both in the nucleus and cytoplasm. Our results demonstrated that following the up-regulated expression of DEFA1B, the levels of ORC1 in whole cell lysis (Fig. 5C) and cytoplasmic protein lysis (Fig. 5D) showed no significant changes compared with the control groups. Interestingly, although DEFA1B was not expressed in the nucleus, the level of ORC1 in nucleus was significantly decreased in DEFA1B -up-regulated cells (Fig. 5E).

3.6. DEFA1B retards the progression of cell cycle

We used flow cytometry to analyze the cellular DNA content to identify the percentage of G1, S and G2/M in the cell cycle. Our data showed 2 days after transfection, the percentage of G2/M in DEFA1B-up-regulated cells was significantly decreased compared with the control groups (Fig. 6A–D). To be able to follow the progression of cell cycle more precisely, we synchronized cultured HEK293T cells with thymidine which is the most commonly used S-phase blocker and its addition to the culture medium depletes nucleotide pools and inhibits

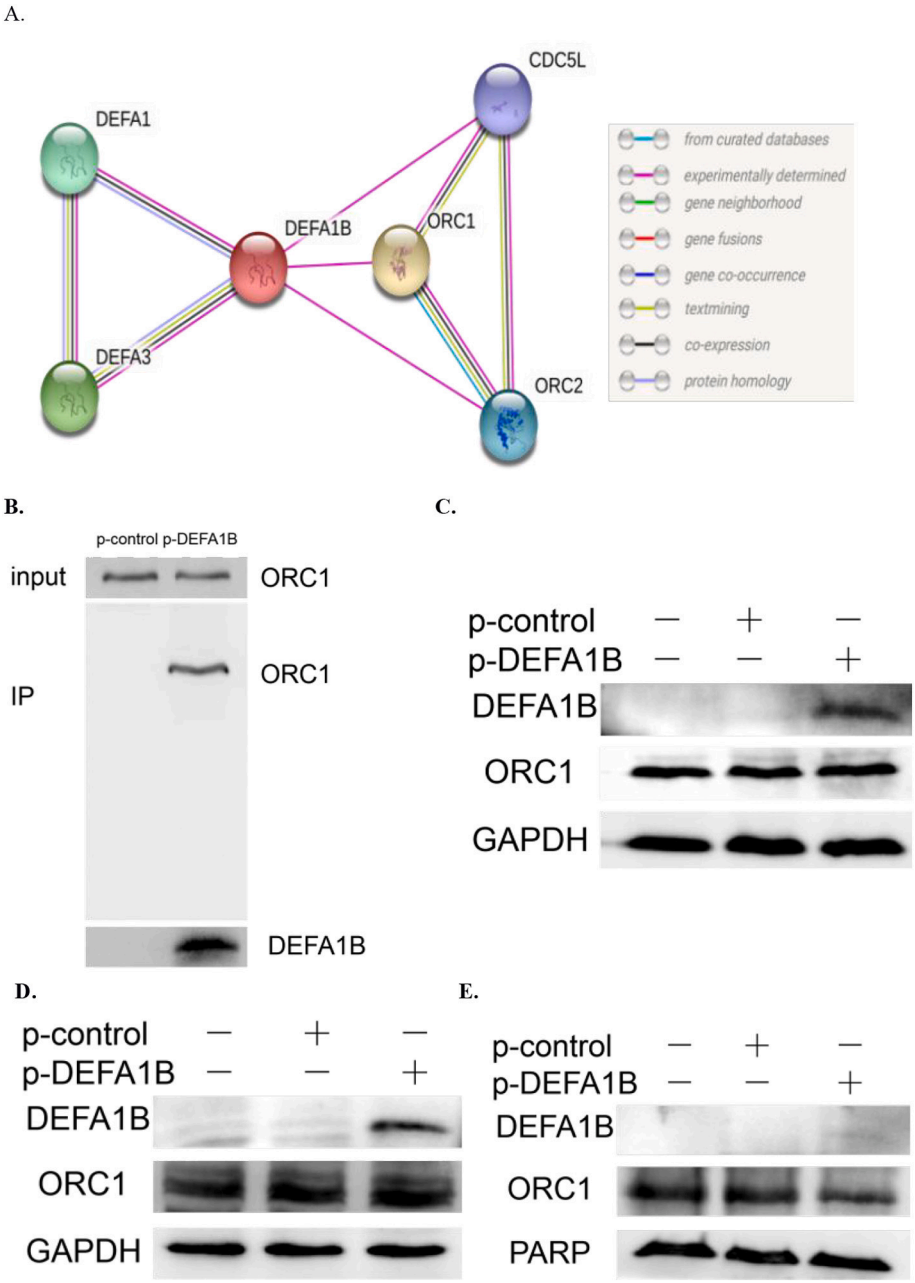

Fig. 5. (A) The protein interaction network was generated using the STRING database. (B) Co-IP data showed DEFA1B interacts with ORC1. HEK293T cells after transfection with the pcDNA3.1-DEFA1B-T2A-EGFP plasmid (pDEFA1B) or pcDNA3.1-T2A-EGFP (vector) or no transfection, and western blot was used to analyze the expression of ORC1 in (C) whole cell lysis, (D) cytoplasm, and (E) nuclear.

new DNA synthesis, causing the slowdown or arrest of S-phase progression [20]. After released into normal medium, cell populations at distinct cell cycle phase were collected at different time points (1–10 h) and the overlapped histograms indicated after about 4–5 h some cells finished S + G2 + M stages and returned to G1 phase. So we compared the velocity to finish S + G2 + M stages through analyzing the percentage of G1. Our data showed with time passing by the cultured cells became more and more asynchronous. 6 h following releasing, the percentage of G1 phase was significantly lower in the DEFA1B-up-regulated group, which indicates that DEFA1B retards cell cycle progression (Fig. 6E).

3.7. ZIKV induced exosomes retard the cell cycle progression of HEK293T and SH-SY5Y cells

The internalization of exosomes is one mechanism of cargo delivery to recipient cells. To examine whether exosomes isolated from ZIKV infected A549 cells can be taken up by HEK293T and SH-SY5Y cells, Exo-ZIKV were labeled with PKH67 dye (green) and added to cultured HEK293T cells. Data from fluorescence microscope suggested that Exo-ZIKV were internalized into recipient cells after 6 h co-culture (Fig. 7A). We further determined whether exosomes can transmit the cell cycle retarding effect of DEFA1B to recipient cells, we discriminated the cell cycles of recipient cells using Flow Cytometry. After co-cultured with Exo-ZIKV for 48 h, the percentage of G2/M in HEK293T cells was decreased compared with cells co-cultured with Exo-A549 (Fig. 7B, C). As expected, Exo-ZIKV was also internalized into SH-SY5Y cells (Fig. 7D)

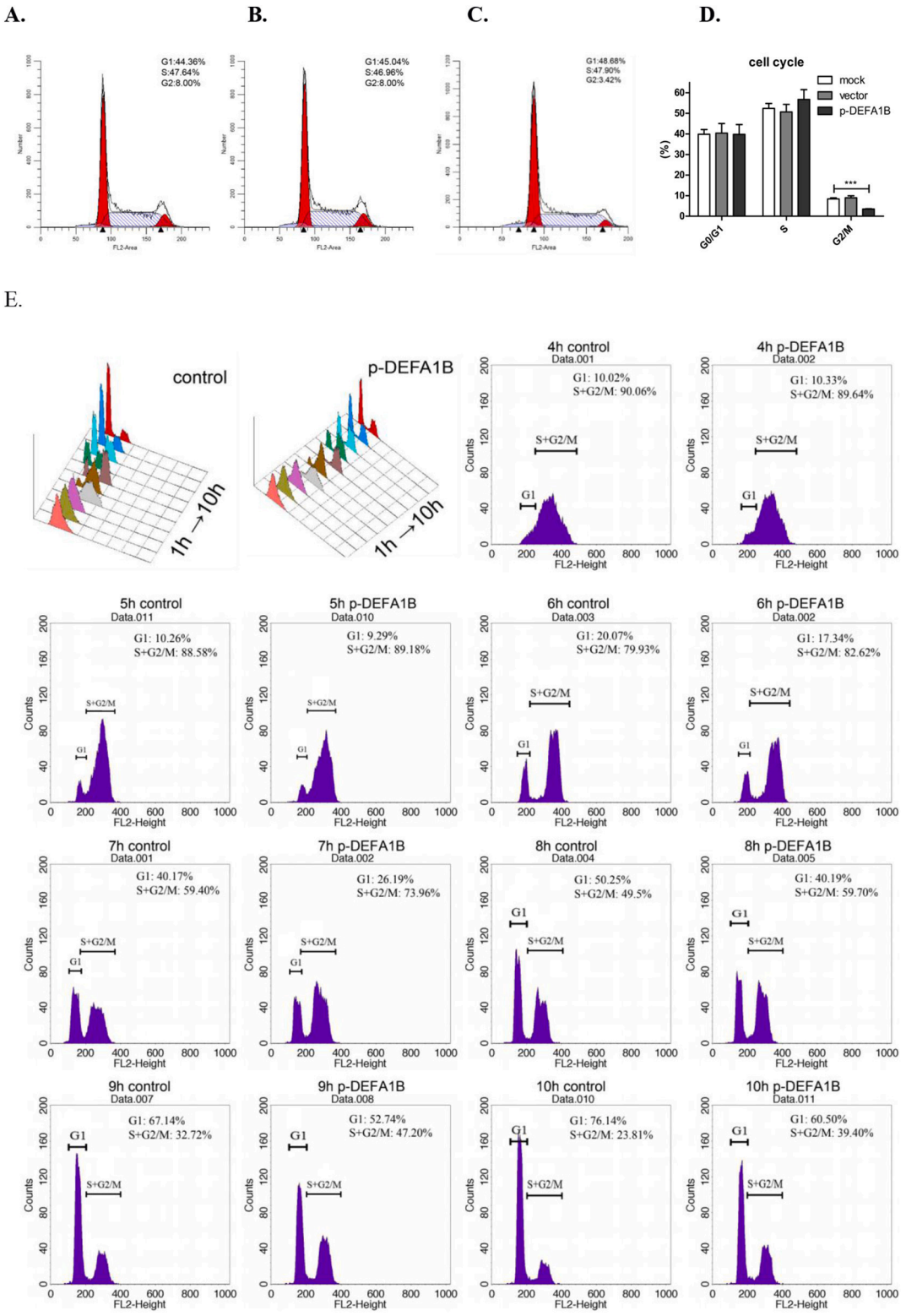

Fig. 6. DEFA1B retards cell cycles. Flow cytometry was used to evaluate the cell cycle progression of the HEK293T cells without transfection (mock) (A) or after transfection with pcDNA3.1-T2A-EGFP (vector) (B) or with the pcDNA3.1-DEFA1B-T2A-EGFP plasmid (pDEFA1B) (C). (D) Statistic analysis of cell cycles after treatment. (E) Cell cycles overlaid histograms showed 1–10 h after release from thymidine, and histograms of cell cycle after release from thymidine from 4 h to 10 h.

and flow cytometry data showed the percentage of G2 of undifferentiated human neuroblastoma SH-SY5Y cells was decreased compared with cells co-cultured with Exo-A549 (Fig. 7E, F).

4. Discussion

Exosomes, as a “carrier” of material and information, play an important role in the interaction between viruses and host cells. Loading functional genes into virus-induced exosomes has been demonstrated to

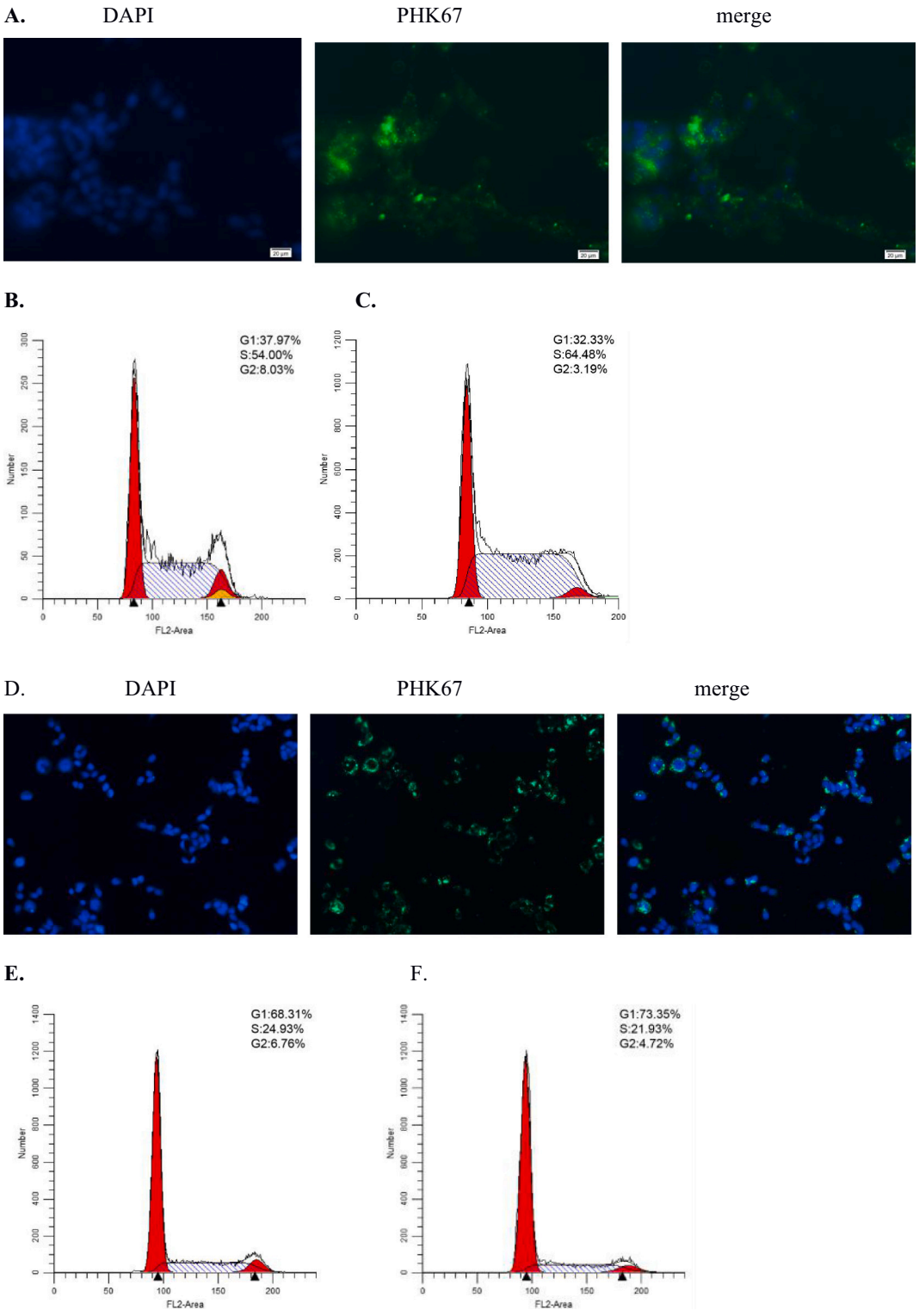

Fig. 7. Exo-ZIKV can be internalized into HEK293T cells after co-cultured for 6 h (A). The cell cycle of HEK293T cells after co-cultured 48 h with Exo-A549 (B) or Exo-ZIKV (C). Exo-ZIKV can be internalized into SH-SY5Y cells after co-cultured for 6 h (D). The cell cycle of SH-SY5Y cells after co-cultured 48 h with Exo-A549 (E) and Exo-ZIKV (F).

modulate viral spread and immune response. In this study, we aimed to understand the role of exosomes in the pathogenesis of ZIKV infection. We first isolated and characterized the exosomes from ZIKV infected/uninfected A549 cells. We showed the exosomes with typical shape, size and protein markers, indicating the vesicles we isolated are indeed exosomes and the isolation method is reliable. Next, we used HTA to identify the differentially-expressed genes between exosomes isolated from ZIKV infected A549 and A549 control cells and we found the expression level of DEFA1B was significantly increased within Exo-ZIKV compared with Exo-A549. To further study the role of DEFA1B in ZIKV replication, we up-regulated the expression level of DEFA1B in A549 cells before infected with ZIKV and the viral replication was assessed by

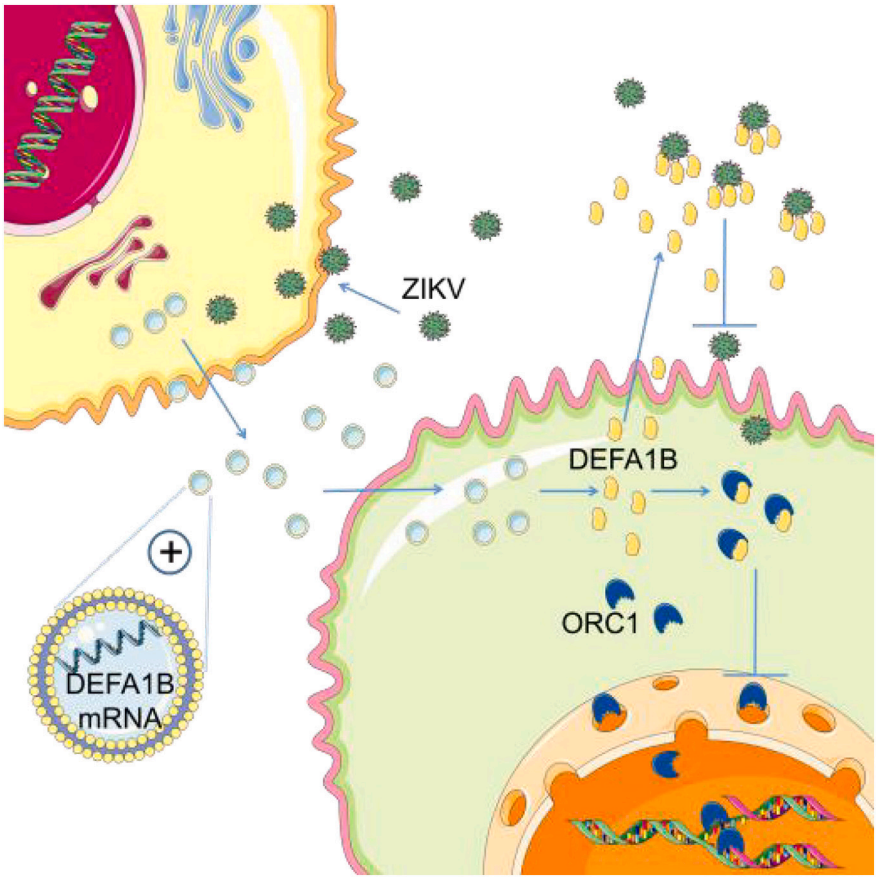

Fig. 8. The mRNA of DEFA1B wrapped in ZIKV-induced exosomes can be internalized into recipient cells. As a secretion protein, DEFA1B inhibits ZIKV before entry step; DEFA1B can also interact with ORC1 in cytoplasm to inhibit ORC1 translocation into nuclear.

RT-PCR and Western Blot. We found extracellular but not the intracellular DEFA1B inhibited ZIKV replication. Surprisingly, we also revealed that DEFA1B could retard the progression of cell cycle. To further explore the underlying mechanism, we identified that DEFA1B interacts with ORC1 to arrest ORC1 entering into the nuclei. In addition, exosomes as carriers can transmit the cell cycle progression retarding effect of DEFA1B into recipient cells, such as SH-SY5Y and 293T cells (Fig. 8).

Human defensins are effector peptides produced by the innate immune system with broad antibacterial, antiviral, and antifungal activities. Defensins are predominantly expressed by neutrophils and can also be expressed by other immune cells and epithelial cells in skin or surfaces in contract with the environment [21]. Our data also showed after ZIKV infection, the DEFA1B increased in host cells as well as in EVs, which can protect from proteinase degradation. Our data showed DEFA1B could be secreted into culture supernatants. Defensins can block viral infection through directly acting on virus particles or indirectly interfering with various stages of the viral life cycle. Available data suggest the antiviral activity of defensins occurs predominantly at viral entry steps; however, antiviral effects at other stages of infection have also been reported, particularly affecting viral trafficking within infected cells [22]. For example, the previous study found that α-Defensin-1 not only had a direct effect on HIV-1 virions but also blocked HIV-1 infection at nuclear import and transcription stages [23]. α-Defensins in supernatants also inhibit the infectivity of HSV-1 and Respiratory Syncytial Virus (RSV) [24]. Our data showed DEFA1B could be secreted into culture supernatants. In addition, the extracellular DEFA1B exerts the anti-ZIKV effect, and the inhibiting effect mainly before ZIKV enter host cells.

In 2015, physicians in Brazil began to report that the number of microcephaly increased among newborns, which was possibly linked to ZIKV infection during the mothers' pregnancy [25–28]. The new emergence of patients with severe nerval system prompted public health emergency of international concerns to explore the suspected association between ZIKV infection and microcephaly. Mouse models showed that ZIKV could destroy the central nerval system to leave severe pathological changes in mice [29]. ZIKV can target human brain cells and ZIKV may impact their survival and growth by restricting the growth of neurospheres and brain organoids [30]. Previous studies found that Meier-Gorlin syndrome patients with mutations in ORC1 had increased microcephaly and a significantly proportionally smaller head circumference and brain [31–33]. Some researchers found that a conserved basic amino acid motif of Orc1 (residues 358–371, Orc1-BP) can specific recognition of thymine residues in the DNA replication origin sequence, and decreased Orc1 in the nuclei could impact the cell growth and be developmentally important [34,35]. In our study we identified that DEFA1B can bind with ORC1 in the cytoplasm and decrease the level of ORC1 in the cell nucleus.

Cell-cycle timings vary markedly during embryo or fetus development, with some stages process rapidly and some stages slow down [36]. For example, in early neurogenesis, neuronal stem cells have a markedly truncated G1 phase in which impaired pre-RC assembly could become rate limiting. As a result of prolonged cell cycle times, even small changes in the number of cell divisions of progenitor and stem cells could have dramatic effects on eventual tissue and organ size [37]. Our data demonstrated that up-regulated DEFA1B expression could significantly retard the progression of cell cycles, and ZIKV induced exosomes internalized into nerve cells (SH-SY5Y cells) and can deliver the detention cell cycle effect. Whether the ZIKV-induced DEFA1B inhibiting cell cycle progression of fetal nerve cells leading to smaller size

of brain needs further investigation.

During human development, the placental barrier blood-brain barriers contribute to fetus brain protection [38]. Although the ZIKV RNA has been detected in amniotic fluid samples, placental tissues and newborn and fetal brain tissues, how the virus crosses the placental and blood-brain barriers remains unclear [39]. Previous studies indicated that exosomes as small transporters can easily get through placental barrier and blood-brain barrier [40,41]. Our data showed the ZIKV induced exosomes could be internalized into recipient cells and inhibit the cells' DNA replication to retard cell cycles.

In summary, our innate immune can increase DEFA1B expression during ZIKV infection, and this can effectively control ZIKV replication. Meanwhile, DEFA1B can retard cell cycles. Because there are some correlations between retarded cell cycles and neurodevelopment. So whether the phenomenon we found linked to the formation of microcephaly? If at the early stage of fetal development, can ZIKV induced exosomes go through the placental barrier and blood-brain barrier to entry fetal brain? Can the DEFA1B within these exosomes inhibit cell cycles of fetal nerve cells and consequence lead to small size of brain? More appropriate animal models may be needed to solve the mystery. It is necessary to find what happened to the fetus and how ZIKV infection generated microcephaly after maternal infection. Also, comparative studies with other similar viruses will also provide experience and lessons. Bioinformatics techniques and findings on similar damages of central nervous system diseases might shed light on the choice of an appropriate animal model, which will be better than cell experiments.

Supplementary data to this article can be found online at https://doi.org/10.1016/j.lfs.2020.118564.

CRediT authorship contribution statement

Shuang Li conceived the study, analyzed the data, and wrote the paper; Anjing Zhu, Kai Ren, Shilin Li and Limin Chen provided experimental materials; Limin Chen revised the paper. All authors have read and agreed to the published version of the manuscript.

Acknowledgements

We acknowledge the technical support by Dr. Wenyu Lin and Dr. Shaobo Wu.

Funding

This work was financially supported by the Chinese Academy of Medical Sciences Innovation Fund for Medical Sciences (2016-12M-3-025, 2017-I2M-B&R-15 to LC); the National Key Research and Development Program (2018YFE0107500 to LC) and Science and Technology Partnership Program (KY201904011 to LC) from Ministry of Science and Technology of China.

Declaration of competing interest

The authors declare no conflicts of interest.

References

[1] N. Wikan, D.R. Smith, Zika virus: history of a newly emerging arbovirus, Lancet Infect. Dis. 16 (2016) e119–e126, https://doi.org/10.1016/S1473-3099(16)30010-X.
[2] D. Baud, D.J. Gubler, B. Schaub, M.C. Lanteri, D. Musso, An update on Zika virus infection, Lancet (London, England) 390 (2017) 2099–2109, https://doi.org/10.1016/S0140-6736(17)31450-2.
[3] H. Tang, C. Hammack, S.C. Ogden, Z. Wen, X. Qian, Y. Li, B. Yao, J. Shin, F. Zhang, E.M. Lee, K.M. Christian, R.A. Didier, P. Jin, H. Song, G.-L. Ming, Zika virus infects human cortical neural progenitors and attenuates their growth, Cell Stem Cell 18 (2016) 587–590, https://doi.org/10.1016/j.stem.2016.02.016.
[4] M.K. Holly, K. Diaz, J.G. Smith, Defensins in viral infection and pathogenesis, Annu. Rev. Virol. 4 (2017) 369–391, https://doi.org/10.1146/annurev-virology-101416-041734.
[5] S.S. Wilson, M.E. Wiens, M.K. Holly, J.G. Smith, Defensins at the mucosal surface: latest insights into defensin-virus interactions, J. Virol. 90 (2016) 5216–5218, https://doi.org/10.1128/JVI.00904-15.
[6] T.L. Chang, J.J. Vargas, A. DelPortillo, M.E. Klotman, Dual role of alpha-defensin-1 in anti-HIV-1 innate immunity, J. Clin. Invest. 115 (2005) 765–773, https://doi.org/10.1172/JCI21948.
[7] A. Ahmed, G. Siman-Tov, G. Hall, N. Bhalla, A. Narayanan, Human antimicrobial peptides as therapeutics for viral infections, Viruses 11 (2019), https://doi.org/10.3390/v11080704.
[8] M.W. Parker, M.R. Botchan, J.M. Berger, Mechanisms and regulation of DNA replication initiation in eukaryotes, Crit. Rev. Biochem. Mol. Biol. 52 (2017) 107–144, https://doi.org/10.1080/10409238.2016.1274717.
[9] M.L. DePamphilis, The “ORC cycle”: a novel pathway for regulating eukaryotic DNA replication, Gene. 310 (2003) 1–15, https://doi.org/10.1016/s0378-1119(03)00546-8.
[10] S.K. Dhar, K. Yoshida, Y. Machida, P. Khaira, B. Chaudhuri, J.A. Wohlschlegel, M. Leffak, J. Yates, A. Dutta, Replication from oriP of Epstein-Barr virus requires human ORC and is inhibited by geminin, Cell 106 (2001) 287–296, https://doi.org/10.1016/s0092-8674(01)00458-5.
[11] Z. Shen, The origin recognition complex in human diseases, Biosci. Rep. 33 (2013), https://doi.org/10.1042/BSR20130036.
[12] L.S. Bicknell, E.M.H.F. Bongers, A. Leitch, S. Brown, J. Schoots, M.E. Harley, S. Aftimos, J.Y. Al-Aama, M. Bober, P.A.J. Brown, H. van Bokhoven, J. Dean, A.Y. Edrees, M. Feingold, A. Fryer, L.H. Hoefsloot, N. Kau, N.V.A.M. Knoers, J. Mackenzie, J.M. Opitz, P. Sarda, A. Ross, I.K. Temple, A. Toutain, C.A. Wise, M. Wright, A.P. Jackson, Mutations in the pre-replication complex cause Meier-Gorlin syndrome, Nat. Genet. 43 (2011) 356–359, https://doi.org/10.1038/ng.775.
[13] S.A. de Munnik, L.S. Bicknell, S. Aftimos, J.Y. Al-Aama, Y. van Bever, M.B. Bober, J. Clayton-Smith, A.Y. Edrees, M. Feingold, A. Fryer, J.M. van Hagen, R.C. Hennekam, M.C.E. Jansweijer, D. Johnson, S.G. Kant, J.M. Opitz, A.R. Ramadevi, W. Reardon, A. Ross, P. Sarda, C.T.R.M. Schrander-Stumpel, J. Schoots, I.K. Temple, P.A. Terhal, A. Toutain, C.A. Wise, M. Wright, D.L. Skidmore, M.E. Samuels, L.H. Hoefsloot, N.V.A.M. Knoers, H.G. Brunner, A.P. Jackson, E.M.H.F. Bongers, Meier-Gorlin syndrome genotype-phenotype studies: 35 individuals with pre-replication complex gene mutations and 10 without molecular diagnosis, Eur. J. Hum. Genet. 20 (2012) 598–606, https://doi.org/10.1038/ejhg.2011.269.
[14] M. Tkach, C. Thery, Communication by extracellular vesicles: where we are and where we need to go, Cell 164 (2016) 1226–1232, https://doi.org/10.1016/j.cell.2016.01.043.
[15] M. Mathieu, L. Martin-Jaular, G. Lavieu, C. Thery, Specificities of secretion and uptake of exosomes and other extracellular vesicles for cell-to-cell communication, Nat. Cell Biol. 21 (2019) 9–17, https://doi.org/10.1038/s41556-018-0250-9.
[16] S. Li, S. Li, S. Wu, L. Chen, Exosomes modulate the viral replication and host immune responses in HBV infection, Biomed. Res. Int. 2019 (2019) 2103943, https://doi.org/10.1155/2019/2103943.
[17] M.S. Vermillion, J. Lei, Y. Shabi, V.K. Baxter, N.P. Crilly, M. McLane, D.E. Griffin, A. Pekosz, S.L. Klein, I. Burd, Intrauterine Zika virus infection of pregnant immunocompetent mice models transplacental transmission and adverse perinatal outcomes, Nat. Commun. (2017), https://doi.org/10.1038/ncomms14575.
[18] W. Zhou, M. Woodson, M.B. Sherman, G. Neelakanta, H. Sultana, Exosomes mediate Zika virus transmission through SMPD3 neutral sphingomyelinase in cortical neurons, Emerg. Microbes Infect. 8 (2019) 307–326, https://doi.org/10.1080/22221751.2019.1578188.
[19] C. Thery, S. Amigorena, G. Raposo, A. Clayton, Isolation and characterization of exosomes from cell culture supernatants and biological fluids, Curr. Protoc. Cell Biol. (2006), https://doi.org/10.1002/0471143030.cb0322s30 Chapter 3. Unit 3.22.
[20] N. Yoshizawa-Sugata, H. Masai, Cell cycle synchronization and flow cytometry analysis of mammalian cells, Methods Mol. Biol. 1170 (2014) 279–293, https://doi.org/10.1007/978-1-4939-0888-2_13.
[21] M. Suarez-Carmona, P. Hubert, P. Delvenne, M. Herfs, Defensins: “simple” antimicrobial peptides or broad-spectrum molecules? Cytokine Growth Factor Rev. 26 (2015) 361–370, https://doi.org/10.1016/j.cytogfr.2014.12.005.
[22] M.E. Selsted, A.J. Ouellette, Mammalian defensins in the antimicrobial immune response, Nat. Immunol. 6 (2005) 551–557, https://doi.org/10.1038/ni1206.
[23] T.L. Chang, J.J. Vargas, A. DelPortillo, M.E. Klotman, Dual role of alpha-defensin-1 in anti-HIV-1 innate immunity, J. Clin. Invest. 115 (2005) 765–773, https://doi.org/10.1172/JCI21948.
[24] F. Chouinard, C. Turcotte, X. Guan, M.-C. Larose, S. Poirier, L. Bouchard, V. Provost, L. Flamand, N. Grandvaux, N. Flamand, 2-Arachidonoyl-glycerol- and arachidonic acid-stimulated neutrophils release antimicrobial effectors against E. coli, S. aureus, HSV-1, and RSV, J. Leukoc. Biol. 93 (2013) 267–276, https://doi.org/10.1189/jlb.0412200.
[25] S. Ioos, H.-P. Mallet, I. Leparc Goffart, V. Gauthier, T. Cardoso, M. Herida, Current Zika virus epidemiology and recent epidemics, Med. Mal. Infect. 44 (2014) 302–307, https://doi.org/10.1016/j.medmal.2014.04.008.
[26] M. Triunfol, A new mosquito-borne threat to pregnant women in Brazil, Lancet Infect. Dis. 16 (2016) 156–157, https://doi.org/10.1016/S1473-3099(15)00548-4.
[27] J. Mlakar, M. Korva, N. Tul, M. Popovic, M. Poljsak-Prijatelj, J. Mraz, M. Kolenc, K. Resman Rus, T. Vesnaver Vipotnik, V. Fabjan Vodusek, A. Vizjak, J. Pizem, M. Petrovec, T. Avsic Zupanc, Zika virus associated with microcephaly, N. Engl. J. Med. 374 (2016) 951–958, https://doi.org/10.1056/NEJMoa1600651.
[28] D. Gatherer, A. Kohl, Zika virus: a previously slow pandemic spreads rapidly through the Americas, J. Gen. Virol. 97 (2016) 269–273, https://doi.org/10.1099/

jgv.0.000381.
[29] F.R. Cugola, I.R. Fernandes, F.B. Russo, B.C. Freitas, J.L.M. Dias, K.P. Guimaraes, C. Benazzato, N. Almeida, G.C. Pignatari, S. Romero, C.M. Polonio, I. Cunha, C.L. Freitas, W.N. Brandao, C. Rossato, D.G. Andrade, D. de P. Faria, A.T. Garcez, C.A. Buchpigel, C.T. Braconi, E. Mendes, A.A. Sall, P.M. de A. Zanotto, J.P.S. Peron, A.R. Muotri, P.C.B. Beltrao-Braga, The Brazilian Zika virus strain causes birth defects in experimental models, Nature 534 (2016) 267–271, https://doi.org/10.1038/nature18296.
[30] P.P. Garcez, E.C. Loiola, R. Madeiro da Costa, L.M. Higa, P. Trindade, R. Delvecchio, J.M. Nascimento, R. Brindeiro, A. Tanuri, S.K. Rehen, Zika virus impairs growth in human neurospheres and brain organoids, Science 352 (2016) 816–818, https://doi.org/10.1126/science.aaf6116.
[31] L.S. Bicknell, S. Walker, A. Klingseisen, T. Stiff, A. Leitch, C. Kerzendorfer, C.-A. Martin, P. Yeyati, N. Al Sanna, M. Bober, D. Johnson, C. Wise, A.P. Jackson, M. O'Driscoll, P.A. Jeggo, Mutations in ORC1, encoding the largest subunit of the origin recognition complex, cause microcephalic primordial dwarfism resembling Meier-Gorlin syndrome, Nat. Genet. 43 (2011) 350–355, https://doi.org/10.1038/ng.776.
[32] A.J. Kuo, J. Song, P. Cheung, S. Ishibe-Murakami, S. Yamazoe, J.K. Chen, D.J. Patel, O. Gozani, The BAH domain of ORC1 links H4K20me2 to DNA replication licensing and Meier-Gorlin syndrome, Nature 484 (2012) 115–119, https://doi.org/10.1038/nature10956.
[33] M. Hossain, B. Stillman, Meier-Gorlin syndrome mutations disrupt an Orc1 CDK inhibitory domain and cause centrosome reduplication, Genes Dev. 26 (2012) 1797–1810, https://doi.org/10.1101/gad.197178.112.
[34] N. Li, W.H. Lam, Y. Zhai, J. Cheng, E. Cheng, Y. Zhao, N. Gao, B.-K. Tye, Structure of the origin recognition complex bound to DNA replication origin, Nature 559 (2018) 217–222, https://doi.org/10.1038/s41586-018-0293-x.
[35] T. Okano-Uchida, L.N. Kent, M.M. Ouseph, B. McCarty, J.J. Frank, R. Kladney, M.C. Cuitino, J.C. Thompson, V. Coppola, M. Asano, G. Leone, Endoreduplication of the mouse genome in the absence of ORC1, Genes Dev. 32 (2018) 978–990, https://doi.org/10.1101/gad.311910.118.
[36] T. Takahashi, R.S. Nowakowski, V.S.J. Caviness, The cell cycle of the pseudostratified ventricular epithelium of the embryonic murine cerebral wall, J. Neurosci. 15 (1995) 6046–6057.
[37] P. Rakic, A small step for the cell, a giant leap for mankind: a hypothesis of neocortical expansion during evolution, Trends Neurosci. 18 (1995) 383–388, https://doi.org/10.1016/0166-2236(95)93934-p.
[38] D. Virgintino, M. Errede, F. Girolamo, C. Capobianco, D. Robertson, A. Vimercati, G. Serio, A. Di Benedetto, Y. Yonekawa, K. Frei, L. Roncali, Fetal blood-brain barrier P-glycoprotein contributes to brain protection during human development, J. Neuropathol. Exp. Neurol. 67 (2008) 50–61, https://doi.org/10.1097/nen.0b013e31815f65d9.
[39] L. de Noronha, C. Zanluca, M.L.V. Azevedo, K.G. Luz, C.N.D. Dos Santos, Zika virus damages the human placental barrier and presents marked fetal neurotropism, Mem. Inst. Oswaldo Cruz 111 (2016) 287–293, https://doi.org/10.1590/0074-02760160085.
[40] S. Nair, C. Salomon, Extracellular vesicles and their immunomodulatory functions in pregnancy, Semin. Immunopathol. 40 (2018) 425–437, https://doi.org/10.1007/s00281-018-0680-2.
[41] J. Matsumoto, T. Stewart, W.A. Banks, J. Zhang, The transport mechanism of extracellular vesicles at the blood-brain barrier, Curr. Pharm. Des. 23 (2017) 6206–6214, https://doi.org/10.2174/1381612823666170913164738.